Author/s:
Russell, IC;Zhang, X;Bumbak, F;McNeill, SM;Josephs, TM;Leeming, MG;Christopoulos, G;Venugopal, H;Flocco, MM;Sexton, PM;Wootten, D;Belousoff, MJ

Title:
Lipid-Dependent Activation of the Orphan G Protein-Coupled Receptor, GPR3

Date:
2024-02-20

Citation:
Russell, I. C., Zhang, X., Bumbak, F., McNeill, S. M., Josephs, T. M., Leeming, M. G., Christopoulos, G., Venugopal, H., Flocco, M. M., Sexton, P. M., Wootten, D. & Belousoff, M. J. (2024). Lipid-Dependent Activation of the Orphan G Protein-Coupled Receptor, GPR3. Biochemistry, 63 (5), pp.625-631. https://doi.org/10.1021/acs.biochem.3c00647.

Persistent Link:
https://hdl.handle.net/11343/358260

Biochemistry

pubs.acs.org/biochemistry
Article

Lipid-Dependent Activation of the Orphan G Protein-Coupled Receptor, GPR3

Isabella C. Russell, Xin Zhang, Fabian Bumbak, Samantha M. McNeill, Tracy M. Josephs, Michael G. Leeming, George Christopoulos, Hariprasad Venugopal, Maria M. Flocco, Patrick M. Sexton,* Denise Wootten,* and Matthew J. Belousoff*

Cite This: *Biochemistry* 2024, 63, 625–631

Read Online

ACCESS | Metrics & More | Article Recommendations | Supporting Information

ABSTRACT: The class A orphan G protein-coupled receptor (GPCR), GPR3, has been implicated in a variety of conditions, including Alzheimer's and premature ovarian failure. GPR3 constitutively couples with Gαs, resulting in the production of cAMP in cells. While tool compounds and several putative endogenous ligands have emerged for the receptor, its endogenous ligand, if it exists, remains a mystery. As novel potential drug targets, the structures of orphan GPCRs have been of increasing interest, revealing distinct modes of activation, including autoactivation, presence of constitutively activating mutations, or via cryptic ligands. Here, we present a cryo-electron microscopy (cryo-EM) structure of the orphan GPCR, GPR3 in complex with DNGαs and G$\beta_1\gamma_2$. The structure revealed clear density for a lipid-like ligand that bound within an extended hydrophobic groove, suggesting that the observed "constitutive activity" was likely due to activation via a lipid that may be ubiquitously present. Analysis of conformational variance within the cryo-EM data set revealed twisting motions of the GPR3 transmembrane helices that appeared coordinated with changes in the lipid-like density. We propose a mechanism for the binding of a lipid to its putative orthosteric binding pocket linked to the GPR3 dynamics.

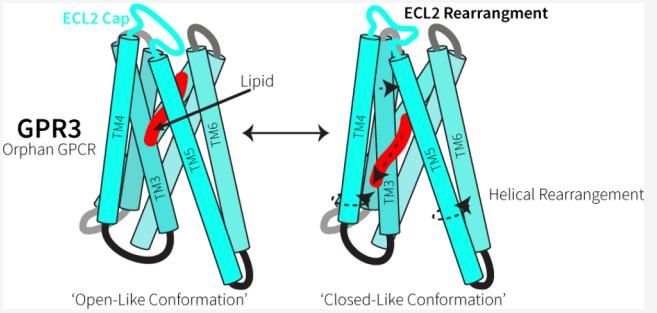

Over 800 G protein-coupled receptors (GPCRs) are encoded for by the human genome, responsible for a wide range of physiological functions and playing a role in disease manifestation and resolution. The importance of these receptors is highlighted by their role as drug targets, with GPCRs comprising ~30% of currently marketed drugs.[1] Despite the considerable interest in GPCRs, the endogenous ligands for around 100 receptors remain unknown; these receptors are termed orphan GPCRs (oGPCRs).[1] GPCRs canonically bind to a G protein heterotrimer (comprising α, β, and γ subunits) to initiate intracellular responses. While agonist binding is traditionally required for G protein association and activation, some GPCRs productively engage G proteins independent of ligand association. This constitutive activity can occur both as a result of specific disease-causing mutations and, in a receptor-dependent manner, as a natural facet of receptor function.[2,3]

GPR3 is a class A oGPCR, expressed in the central nervous system and adipose tissues.[2] GPR3 has been linked to a variety of conditions, including Alzheimer's, due to its impact on β-amyloid production through β-arrestin recruitment;[4] premature ovarian failure, where the high cAMP production of GPR3 in oocytes holds them in meiotic arrest;[5] and an impact on addiction[6] and pain in nerve injury.[7] Recent data suggests that the physiological activity of GPR3 may primarily be driven by constitutive signaling, with regulation of GPR3 responses achieved through changes to receptor expression. For example, GPR3 expression is upregulated in brown adipose tissue in mice in response to cold temperatures.[2,8] Although tool compounds and potential ligands for this receptor have been proposed, no endogenous ligands have been validated.[9]

Here, we validated the previously reported constitutive activity of GPR3[10] in direct assays of Gs protein coupling (Figure 1A) and in a downstream cAMP accumulation assay (Figure 1B). Despite this, GPR3 exhibits strong sequence conservation within class A activation motifs that are perturbed in many constitutively active receptors[3] (Figure 1C). This suggests that GPR3 constitutive activity may arise from the presence of an autoactivation domain or an endogenous prebound ligand. Indeed, previous mutagenesis studies on GPR3 have hypothesized autoactivation by the N terminus,

Received: November 18, 2023
Revised: February 2, 2024
Accepted: February 12, 2024
Published: February 20, 2024

https://doi.org/10.1021/acs.biochem.3c00647
Biochemistry 2024, 63, 625–631

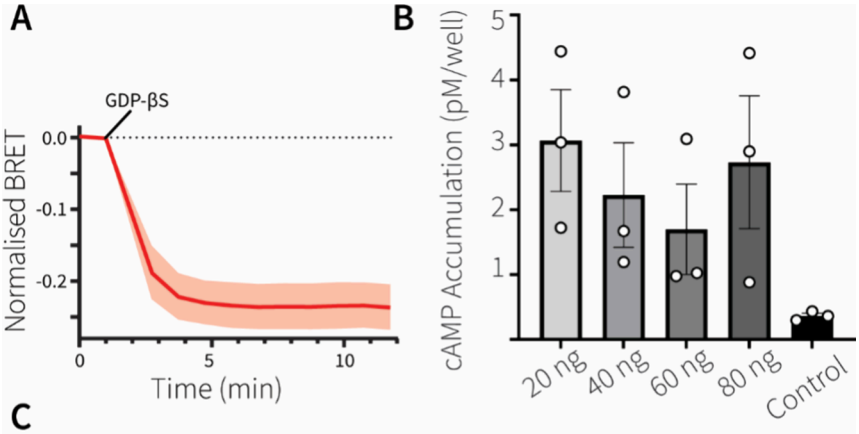

	P5.50	I3.40	F6.44	D3.49	R3.50	Y3.51	C6.47	W6.48	P6.50
GPR3	V	I	F	D	R	Y	C	W	P
GPR12	M	V	F	D	R	Y	C	W	P
β1AR	P	I	F	D	R	Y	C	W	P
S1P1R	L	V	F	E	R	Y	C	W	P

Figure 1. (A) Normalized bioluminescence resonance energy transfer (BRET) between Rluc8-tagged GPR3 and split-Venus tagged $G\beta_1\gamma_2$. Upon addition of GDP-βs (100 μM; black line) to apyrase-treated permeabilized cells, the constitutively active receptor stimulates turnover of the precomplexed $G\alpha_s$ heterotrimer. $G\alpha_s$ heterotrimer dissociation from the receptor is indicated by the reduction in the BRET ratio due to separation of the Venus and Rluc8 tags.[10] BRET ratios (ΔBRET) were baseline corrected twice. First, the average of the first two data points was subtracted from the data points of each individual experiment. Second, the values from experiments where no GDP-βs was added were subtracted from the corresponding values of experiments where GDP-βs was added after the second baseline read. The data shown in panel A represent the average ($\pm$ SEM) difference from the baseline of four independent experiments (n = 4), each performed in technical duplicate. (B) Basal cAMP accumulation over 60 min expressed as pM/well. HEK293a cells were transiently transfected in suspension with a tagged GPR3 or pcDNA3.1 vector control. Data shown as the means $\pm$ SEM where n = 3 independent experiments with individual mean experimental data points displayed. (C) Sequence comparison of key conserved class A GPCR motifs. The related orphan receptors, GPR3 and GPR12, are compared to the prototypical class A GPCR, β1-adrenoreceptor (β1AR), and the related lipid receptor, sphingosine-1-phosphate-receptor 1 (S1P1R). Residues are color coded as follows: red, acidic/negatively charged; orange, aliphatic; yellow, aromatic; green, polar/neutral; blue, basic/positively charged. Sequence comparison was performed using GPCRdb (www.gpcrdb.org), and aligned residues are numbered using the Ballesteros–Weinstein numbering system.[12]

while other studies have indicated that it may respond to the presence of endogenous lipids, such as sphingosine-1-phosphate, resulting in the observed high basal signaling.[2,11] However, structural information is required to understand the underlying mechanism of GPR3 activation.

Contemporary structural studies of class A oGPCRs have uncovered distinct modes of activation, particularly for receptors with known constitutive activity. Some receptors, such as GPR52, undergo autoactivation, where extracellular loop 2 (ECL2) dips deeply into the transmembrane domain (TMD) core, forming contacts with conserved motifs implicated in ligand-mediated receptor activation.[13] For other oGPCRs, resolved structures have revealed the presence of a cryptic ligand, such as that observed in GPR119, where a lipid activator was copurified in the active complex.[14]

To understand the activation of GPR3, we determined a cryo-electron microscopy (cryo-EM) structure of the receptor in complex with dominant negative (DN) $G\alpha_s$ and $G\beta_1\gamma_2$ (Figure 2A). Briefly, GPR3, DN$G\alpha_s$, and $G\beta_1\gamma_2$ were coexpressed in *Trichoplusia ni* cells using a *baculovirus* expression vector at a 4:2:1 ratio followed by addition of nanobody 35 (Nb35). The active GPR3 complex was purified by Flag affinity chromatography, followed by size exclusion chromatography; peaks containing complex particles were pooled and concentrated for cryo-EM imaging (Figure S2A–E). Following iterative rounds of classification and refinement (Figure S3), the structure was resolved to 3.5 Å (Figure S4). Of note, while the complex was copurified with Nb35 (Figure S2B), no density was present for the nanobody in the refined maps, suggesting that the conformation of a GPR3-bound $G\alpha_s$ protein had diminished affinity for Nb35 (see supplemental discussion).

The structure revealed an ECL2 "cap" (Figure 2B), reminiscent of those reported in the structures of lipid receptors, such as the sphingosine-1-phosphate receptor (S1P1R).[15] The ECL2 cap in GPR3 stabilizes binding of a lipid that appears to extend through a hydrophobic channel in the receptor core to an exit between TM4/5 near the intracellular side of the receptor (Figure 2C,D). The lipid-bound hydrophobic pocket within the receptor originates below ECL2 and terminates near V205$^{5.50}$ of the PIF motif, although additional discontinuous density can be observed below this. At low thresholds, this lower lipid-like density can be observed in proximity to hydrophobic residues at the intracellular side of the receptor, including L128$^{3.44}$, L159$^{4.48}$, and M156$^{4.45}$ among others (Figure 2C).

CryoSPARC 3D variability analysis (3DVA) of principal components of motion within the EM data revealed a transition between two distinct receptor conformations (Figure 3A,B; Supplementary Video). While lipid-like density is

https://doi.org/10.1021/acs.biochem.3c00647
Biochemistry 2024, 63, 625–631

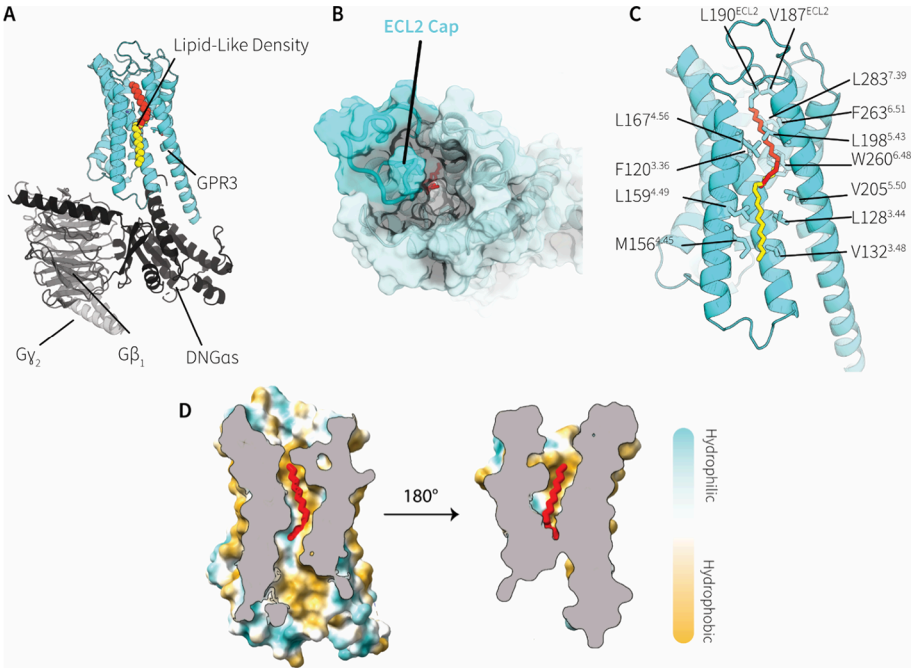

Figure 2. (A) Cryo-EM structure of GPR3:DNGα_s:G$\beta_1\gamma_2$. GPR3: cyan, lipid: red, DNGα_s: black, Gβ1: dark gray, Gγ_2: light gray. (B) The placement of ECL2, as well as the extracellular portion of the TMD, largely occludes access to the intracellular domain, although a small entrance can still be observed. (C) Model of potential lipid(s) in the TM cavity. The lipid was modeled as a simple 16 carbon saturated lipid, with two individual lipids modeled (red and yellow) to account for the extended density in the cryo-EM map. Receptor residues that are in the proximity of the lipid are represented as sticks. These residues create a hydrophobic "channel" where the lipid is proposed to bind. These residues include key class A activation motifs: the PIF motif and the W$^{6.48}$ toggle switch. (D) Hydrophobic surface representation of the GPR3, including the placement of the lipid in its "upper" position.

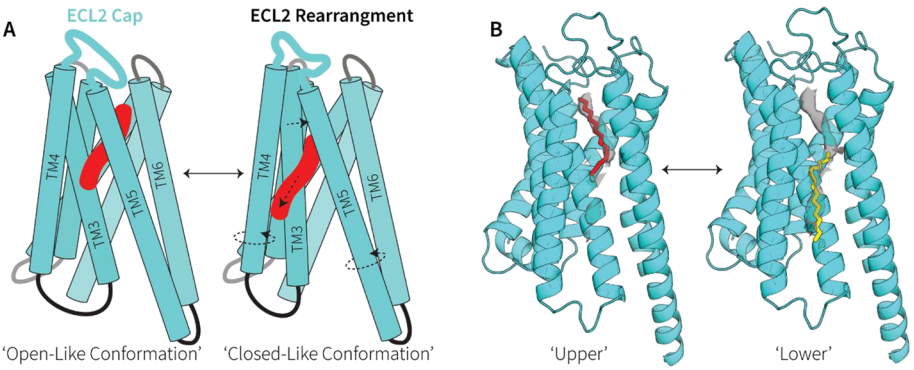

Figure 3. (A) Cartoon schematic illustrating the rearrangement of the ECL2 and TMD observed in the 3DVA (further details supplied in the legend for Supplementary Video 1). (B) Placement of the lipid in its "upper" position (left) and its "lower" position (right).

present throughout the transition, the density is very dynamic, suggesting that the lipid may be moving in concert with changes in receptor conformation. Within the receptor, there is coordinated reorganization of the TM bundle and ECL2 between "open-like" and "closed-like" conformations. In the open-like conformation, the extracellular sides of TM3 and TM6/ECL3/TM7 are further apart, supporting positioning of the lipid in the upper hydrophobic groove, with ECL2 capping this pocket. As the receptor transitions to the closed conformation, ECL2 shifts away from the ligand pocket, while the extracellular ends of TM3 and ECL3 move toward ECL2, contracting the upper binding pocket. These changes are accompanied by an apparent clockwise rotation of TMs 4, 5, and 7 (Figure 3A). The residues within the hydrophobic groove rotate with their TMs, resulting in rearrangement of I124$^{3.40}$ and V205$^{5.50}$ of the PIF motif (VIF in GPR3), which sit along the proposed binding pocket of the lipid (Figure 2C). While speculative, these conformational changes could be involved in the process of lipid engagement/disengagement.

The lower lipid-like density was evident in both the "open" and "closed" conformations; however, it was more prominent in the latter. Furthermore, while the lipid-like density is contiguous in low-contour maps, it is discontinuous at a high contour. As such, it is possible that the lipid is either a long-chain fatty acid or a shorter lipid undergoing entry and egress from the receptor where it is metastably engaged at multiple points along this path. A caveat of the 3DVA is the relatively small number of particles available for serial map reconstruction that could also contribute to the variance in resolution of the lipid density. When modeled into the consensus map as two simple saturated 16 carbon chain molecules, higher

https://doi.org/10.1021/acs.biochem.3c00647
Biochemistry 2024, 63, 625−631

occupancy is predicted, using Coot, for the lipid in the "upper" portion of the receptor (Figure 3B).

To explore the potential identity of the lipid-like density in the structure, active GPR3-Gs complexes were purified and subjected to lipid extraction, and an extensive semiquantitative mass spectrometric analysis was conducted. A total of 158 lipid molecules, encompassing two major lipid categories, fatty acids (FA) and triglycerides (TG), spanning 20 lipid classes, were identified and semiquantified at the "sum composition" level (Figure S5). At this level, the lipid class, subclass, total number of carbon atoms, and total number of C═C double bonds in the fatty acyl-alkyl-alkenyl moieties are determined. For instance, FA 18:2 denotes a linoleic acid with a total of 18 carbons and two double bonds in the acyl chains. The highest enrichment of lipids was seen for FAs between 14 and 22 carbons in length that were either unsaturated, monosaturated, or disaturated (Figure S6). Each of these could be robustly modeled into the EM density, consistent with the potential for GPR3 to be activated by fatty acids (Figure S7). Nonetheless, further work is required to determine the identity of the endogenous lipid activator as well as to explore the role of TM movements on lipid binding and receptor activation.

A comparable lipid binding pocket to that observed in GPR3 can be seen in GPR119, an orphan receptor that putatively binds to lysophosphatidylcholine (LPC) as its endogenous ligand, as well as S1P1R, which is activated by the lipid, sphingosine-1-phosphate (S1P) (Figure 4A,B). A similar binding mode is also observed in GPR174 that putatively binds lysophosphatidylserine (LysoPS). GPR119, while exhibiting an extended lipid density similar to GPR3, binds to a phospholipid whose headgroup extends beyond ECL2, forming extensive hydrophilic and polar interactions with the receptor extracellular domain and ECLs, resulting in outward shifts of TM1 and ECL3 when compared to GPR3 (Figure 4B).[14] Moreover, ECL2 also adopts a conformation different from that in GPR3, and GPR119 engages with the lipid tail via a distinct series of amino acids within the hydrophobic channel (Figure S8). GPR174 also features an extended binding pocket that traverses the lipid bilayer; however, there are distinct differences in the extracellular region, including in the placement of ECL2 (Figure 4D).[16] Additionally, GPR174 has a pronounced kink in TM5, which results in differential placement of the lipid in its binding pocket.

S1P1R binds to its endogenous lipid in a similar extended hydrophobic groove to GPR3 and GPR119, with the lipid tail traversing the TMD (Figure 4A). The hydrophilic headgroup is accommodated by hydrophilic residues in an extracellular vestibule of the binding pocket, and its hydrophobic acyl chain is surrounded by hydrophobic residues, many of which are conserved with GPR3, including $F^{5.47}$, $F(GPR3)^{3.36}L(S1P1R)$, and $F(GPR3)^{6.51}L(S1P1R)$. Similar to GPR119, the extracellular region of S1P1R displays a conformation distinct from that of GPR3 to accommodate the phosphate headgroup (Figure 4A). While S1P has been proposed as a potential ligand for GPR3, it is clear from our maps that there is no density that would support the presence of a hydrophilic phosphate headgroup, and substantial structural changes would be required to enable binding of S1P, suggesting that it is unlikely to be the primary endogenous ligand for GPR3.

Our data is consistent with an important role for ECL2 in capping the lipid binding pocket and in stabilization of the lipid in the upper hydrophobic pocket in the absence of polar interactions that would support phospholipid binding. A capping motif has been observed in the active structures of other lipid receptors, including CB1R (Figure 4C), suggesting that this may be an important conserved feature for stabilizing lipid agonists. GPR3 is a member of an oGPCR subfamily consisting of GPRs 3, 6, and 12. GPRs 6 and 12 have also been predicted to bind to cannabinoid and sphingosine-related lipids,[9] and, similar to GPR3, they retain most of the conserved class A activation motifs, with the "PIF" motif being the least conserved (Figure 1C). Recently, a constitutively active, $G\alpha_s$ protein-bound structure of GPR12 was reported.[17] In that study, GPR12 was proposed to undergo autoactivation via TMD engagement of ECL2 due to a lack of robust evidence for a cryptic agonist ligand.

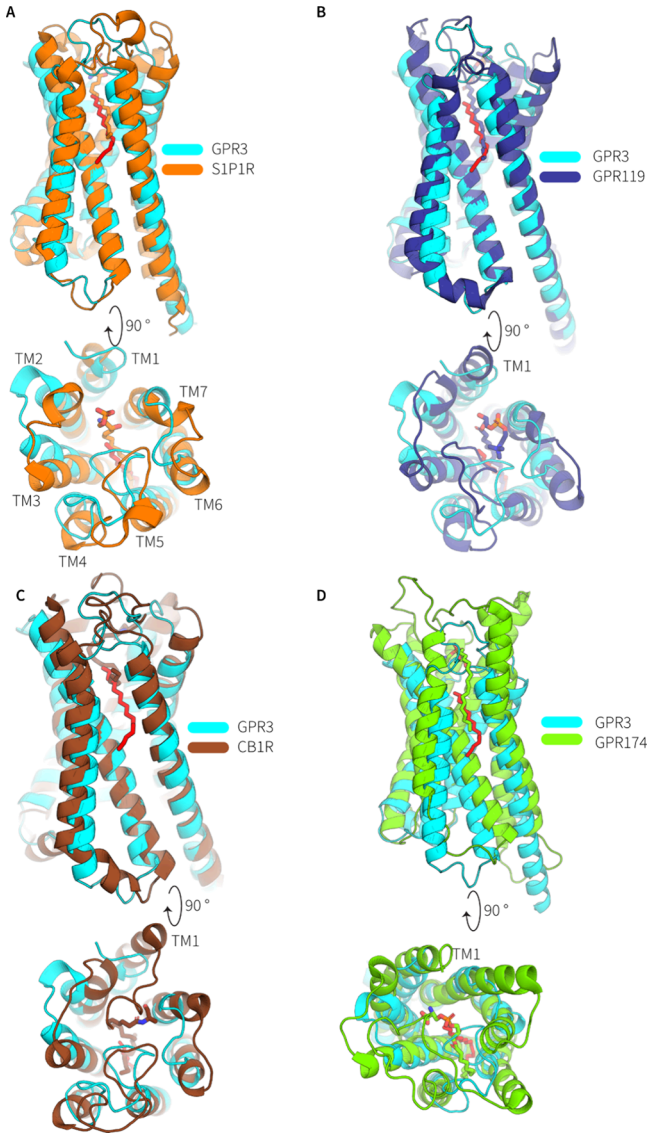

Figure 4. Side and top views of GPR3 superimposed with similar lipid binding receptors. (A) S1P1R with its endogenous lipid S1P (PDB: 7VIE). (B) GPR119 with its endogenous lipid (PDB: 7XZ5). (C) CB1R was bound to an endocannabinoid-like analogue (PDB: 8GHV). (D) GPR174 was bound to the endogenous lipid LPC (7XV3). The placement of the TMs is equivalent in each panel. In all comparisons, the modeled lipid in GPR3 is colored red, with the backbone of the ligands present in the comparator structures color matched to the receptor.

https://doi.org/10.1021/acs.biochem.3c00647
Biochemistry 2024, 63, 625−631

There is a strong correlation between the backbone conformations of GPR12 and GPR3 (Figure S9), including overlap in the conformation of ECL2, suggesting that these receptors likely share a similar mechanism for activation. Moreover, the position of ECL2 is relatively shallow and distinct from those of autoactivated receptors such as GPR52 where ECL2 penetrates deep into the TM bundle, a pose that overlaps the orthosteric binding pocket of many class A GPCRs, including the upper lipid pocket of GPR3. Examination of the GPR12 model reveals an open cavity beneath ECL2, and there is also a weak density within this cavity in the deposited EM map (Figure S9A). Collectively, we believe that GPR12 is unlikely to be an autoactivated GPCR but rather activated by a cryptic ligand, similar to GPR3, although there is limited ability to resolve the ligand density due to the low number of particles in the deposited final map. However, further studies are required to validate this hypothesis.

In conclusion, this work presents the novel structure of GPR3, an elusive oGPCR, in complex with the DNGα_s and G$\beta_1\gamma_2$ subunits. We reveal that GPR3 is a lipid-activated receptor, with the previously described constitutive activity of the receptor likely due to high occupancy of the receptor by an endogenous lipid(s) that is likely to be a fatty acid(s). Additionally, 3DVA of active complex provided potential mechanistic insight into entry/egress of the lipid that may be linked to receptor activation. This work provides key information for understanding the biology of GPR3 and extends our knowledge of GPCR activation mechanisms.

Note, added in proof: At the time of submission of our revised manuscript 2 x articles reporting substantially similar results were published[18,19]

■ ASSOCIATED CONTENT

Data Availability Statement

Atomic coordinates and cryo-EM density map generated in this study are available at the protein databank (https://www.rcsb.org/) under accession code 8U8F and the electron microscopy databank (https://www.ebi.ac.uk/emdb/) under accession code EMD-42023.

Supporting Information

The Supporting Information is available free of charge at https://pubs.acs.org/doi/10.1021/acs.biochem.3c00647.

Additional discussion, supplementary video legend, cell surface expression of GPR3 constructs in mammalian cells, GPR3:Gs complex purification, cryo-EM data processing and EM map resolution, mass spectrometry analysis of lipids, modeling of fatty acids into the GPR3 lipid-like density, GPR3 and GPR119 comparison, GPR3 and GPR12 comparison, cryo-EM data statistics, materials and methods, and methods specific references (PDF)

Cryo-EM conformational dynamics (MP4)

■ AUTHOR INFORMATION

Corresponding Authors

Patrick M. Sexton − *Drug Discovery Biology Theme, Monash Institute of Pharmaceutical Sciences, Monash University, Parkville 3052 Victoria, Australia; Australian Research Council Centre for Cryo-Electron Microscopy of Membrane Proteins, Monash Institute of Pharmaceutical Sciences, Monash University, Parkville 3052 Victoria, Australia;* orcid.org/0000-0001-8902-2473; Email: patrick.sexton@monash.edu

Denise Wootten − *Drug Discovery Biology Theme, Monash Institute of Pharmaceutical Sciences, Monash University, Parkville 3052 Victoria, Australia; Australian Research Council Centre for Cryo-Electron Microscopy of Membrane Proteins, Monash Institute of Pharmaceutical Sciences, Monash University, Parkville 3052 Victoria, Australia;* orcid.org/0000-0003-4563-1642; Email: denise.wootten@monash.edu

Matthew J. Belousoff − *Drug Discovery Biology Theme, Monash Institute of Pharmaceutical Sciences, Monash University, Parkville 3052 Victoria, Australia; Australian Research Council Centre for Cryo-Electron Microscopy of Membrane Proteins, Monash Institute of Pharmaceutical Sciences, Monash University, Parkville 3052 Victoria, Australia;* orcid.org/0000-0002-3229-474X; Email: matthew.belousoff@monash.edu

Authors

Isabella C. Russell − *Drug Discovery Biology Theme, Monash Institute of Pharmaceutical Sciences, Monash University, Parkville 3052 Victoria, Australia; Australian Research Council Centre for Cryo-Electron Microscopy of Membrane Proteins, Monash Institute of Pharmaceutical Sciences, Monash University, Parkville 3052 Victoria, Australia*

Xin Zhang − *Drug Discovery Biology Theme, Monash Institute of Pharmaceutical Sciences, Monash University, Parkville 3052 Victoria, Australia; Australian Research Council Centre for Cryo-Electron Microscopy of Membrane Proteins, Monash Institute of Pharmaceutical Sciences, Monash University, Parkville 3052 Victoria, Australia*

Fabian Bumbak − *Drug Discovery Biology Theme, Monash Institute of Pharmaceutical Sciences, Monash University, Parkville 3052 Victoria, Australia; Australian Research Council Centre for Cryo-Electron Microscopy of Membrane Proteins, Monash Institute of Pharmaceutical Sciences, Monash University, Parkville 3052 Victoria, Australia;* orcid.org/0000-0003-2739-8197

Samantha M. McNeill − *Drug Discovery Biology Theme, Monash Institute of Pharmaceutical Sciences, Monash University, Parkville 3052 Victoria, Australia*

Tracy M. Josephs − *Drug Discovery Biology Theme, Monash Institute of Pharmaceutical Sciences, Monash University, Parkville 3052 Victoria, Australia; Australian Research Council Centre for Cryo-Electron Microscopy of Membrane Proteins, Monash Institute of Pharmaceutical Sciences, Monash University, Parkville 3052 Victoria, Australia;* orcid.org/0000-0002-7799-3683

Michael G. Leeming − *Bio21 Molecular Science & Biotechnology Institute, Melbourne Mass Spectrometry and Proteomics Facility, The University of Melbourne, Melbourne, VIC 3052, Australia*

George Christopoulos − *Drug Discovery Biology Theme, Monash Institute of Pharmaceutical Sciences, Monash University, Parkville 3052 Victoria, Australia*

Hariprasad Venugopal − *Ramaciotti Centre for Cryo Electron Microscopy, Monash University, Clayton 3800 Victoria, Australia*

Maria M. Flocco − *Mechanistic and Structural Biology, Discovery Sciences, BioPharmaceuticals R&D, AstraZeneca, Cambridge CB20AA, United Kingdom*

Complete contact information is available at:

https://pubs.acs.org/10.1021/acs.biochem.3c00647

Author Contributions

The manuscript was written through contributions of all authors. All authors have given approval to the final version of the manuscript. I.C.R. expressed and purified the receptor complex, performed cAMP assays and flow cytometry and analyzed data, imaged sample, and performed cryo-EM data processing and structure determination. G.C. designed and cloned constructs. F.B. prepared baculovirus. F.B. and S.M. performed BRET assays and analyzed data. M.J.B. assisted with cryo-EM data collection, data processing, and molecular modeling. X.Z. vitrified samples and provided supervision and training of I.C.R. T.J.M. and M.G.L. performed and analyzed mass spectrometry experiments. H.V. collected additional cryo-EM data sets. I.C.R., M.J.B., and P.M.S. contributed to data interpretation as well as figure and manuscript preparation. D.W. and P.M.S. designed the project and provided supervision. I.C.R., M.J.B., and P.M.S. generated figures and/or wrote the manuscript. All authors reviewed and edited the manuscript.

Funding

This work was supported by an Australian National Health and Medical Research Council (NHMRC) program grant (#1150083; P.M.S.). P.M.S. is an NHMRC Senior Principal Research Fellow (grant ID: 1154434). D.W. is an NHMRC Senior Research Fellow (grant ID: 1155302). T.M.J. is an NHMRC Emerging Leader Fellow (grant ID: 2008341). X.Z. is an Australian Research Council (ARC) DECRA Fellow (grant ID: DE230101681). P.M.S. is the director, and D.W. is the Monash University Node leader of the ARC Industrial Transformation Training Centre for Cryo-electron Microscopy of Membrane Proteins (CCeMMP) (grant ID: IC200100052), which received support from AstraZeneca for the current project.

Notes

The authors declare the following competing financial interest(s): P.M.S. is a co-founder and shareholder of Septerna Inc. and DACRA Tx. D.W. is a shareholder in Septerna Inc. and co-founder and shareholder of DACRA Tx. M.M.F. is an employee of AstraZeneca.

■ ACKNOWLEDGMENTS

This work was supported by resources from the Bio21 Institute Ian Holmes Imaging Centre, the Monash Massive M3 computational infrastructure, and the Monash Ramaciotti Centre for Cryo-Electron Microscopy. We acknowledge the use and assistance of the Bio21 Mass Spectrometry and Proteomics Facility at the University of Melbourne.

■ ABBREVIATIONS

GPCR, G protein-coupled receptor; oGPCR, orphan G protein-coupled receptor; ECL2, extracellular loop 2; TMD, transmembrane domain; DN, dominant negative; Nb35, nanobody 35; S1P1R, sphingosine-1-phosphate receptor; 3DVA, CryoSPARC 3D variability analysis; UPLC-MS/MS, ultrahigh performance liquid chromatography tandem mass spectrometry; Cer, ceramide; FAHFA, fatty acid hydroxy fatty acid; LPC, lysophosphatidylcholine; LPE, lysophosphatidylethanolamine; PA, phosphatidic acid; PC, phosphatidylcholine; PE, phosphatidylethanolamine; PI, phosphatidylinositol; ASG, alkylsphingosine; CE, cholesteryl ester; DG, diacylglycerol; HBMP, hydroxybutyrate monopalmitin; MG, monoacylglycerol; NAE, *N*-acylethanolamine; NaOrn, *N*-acylornithine; SM, sphingomyelin; PPB, sphingophosphonolipid B; ST, sterol lipid; TG, triglyceride.

■ REFERENCES

(1) Sriram, K.; Insel, P. A. G protein-coupled receptors as targets for approved drugs: how many targets and how many drugs? *Molecular pharmacology* **2018**, *93*, 251−258.

(2) Sveidahl Johansen, O.; Ma, T.; Hansen, J. B.; Markussen, L. K.; Schreiber, R.; Reverte-Salisa, L.; Dong, H.; Christensen, D. P.; Sun, W.; Gnad, T.; Karavaeva, I.; Nielsen, T. S.; Kooijman, S.; Cero, C.; Dmytriyeva, O.; Shen, Y.; Razzoli, M.; O'Brien, S. L.; Kuipers, E. N.; Nielsen, C. H.; Orchard, W.; Willemsen, N.; Jespersen, N. Z.; Lundh, M.; Sustarsic, E. G.; Hallgren, C. M.; Frost, M.; McGonigle, S.; Isidor, M. S.; Broholm, C.; Pedersen, O.; Hansen, J. B.; Grarup, N.; Hansen, T.; Kjær, A.; Granneman, J. G.; Babu, M. M.; Calebiro, D.; Nielsen, S.; Rydén, M.; Soccio, R.; Rensen, P. C. N.; Treebak, J. T.; Schwartz, T. W.; Emanuelli, B.; Bartolomucci, A.; Pfeifer, A.; Zechner, R.; Scheele, C.; Mandrup, S.; Gerhart-Hines, Z. Lipolysis drives expression of the constitutively active receptor GPR3 to induce adipose thermogenesis. *Cell* **2021**, *184*, 3502−3518.

(3) Zhou, Q.; Yang, D.; Wu, M.; Guo, Y.; Guo, W.; Zhong, L.; Cai, X.; Dai, A.; Jang, W.; Shakhnovich, E. I.; Liu, Z.-J.; Stevens, R. C.; Lambert, N. A.; Babu, M. M.; Wang, M.-W.; Zhao, S. Common activation mechanism of class A GPCRs. *eLife* **2019**, *8*, No. e50279.

(4) Huang, Y.; Rafael Guimarães, T.; Todd, N.; Ferguson, C.; Weiss, K. M.; Stauffer, F. R.; McDermott, B.; Hurtle, B. T.; Saito, T.; Saido, T. C.; MacDonald, M. L.; Homanics, G. E.; Thathiah, A. G protein−biased GPR3 signaling ameliorates amyloid pathology in a preclinical Alzheimer's disease mouse model. *Proc. Natl. Acad. Sci. U. S. A.* **2022**, *119*, No. e2204828119.

(5) Vaccari, S.; Horner, K.; Mehlmann, L. M.; Conti, M. Generation of mouse oocytes defective in cAMP synthesis and degradation: Endogenous cyclic AMP is essential for meiotic arrest. *Dev. Biol.* **2008**, *316*, 124−134.

(6) Tourino, C.; Valjent, E.; Ruiz-Medina, J.; Herve, D.; Ledent, C.; Valverde, O. The orphan receptor GPR3 modulates the early phases of cocaine reinforcement. *British journal of pharmacology* **2012**, *167*, 892−904.

(7) Ruiz-Medina, J.; Ledent, C.; Valverde, O. GPR3 orphan receptor is involved in neuropathic pain after peripheral nerve injury and regulates morphine-induced antinociception. *Neuropharmacology* **2011**, *61*, 43−50.

(8) Godlewski, G.; Jourdan, T.; Szanda, G.; Tam, J.; Resat, C.; Harvey-White, J.; Liu, J.; Mukhopadhyay, B.; Pacher, P.; Ming Mo, F.; Osei-Hyiaman, D.; George, K. Mice lacking GPR3 receptors display late-onset obese phenotype due to impaired thermogenic function in brown adipose tissue. *Sci. Rep.* **2015**, *5*, 14953.

(9) Ye, C.; Zhang, Z.; Wang, Z.; Hua, Q.; Zhang, R.; Xie, X. Identification of a novel small-molecule agonist for human G protein−coupled receptor 3. *Journal of Pharmacology and Experimental Therapeutics* **2014**, *349*, 437−443.

(10) Lu, S.; Jang, W.; Inoue, A.; Lambert, N. A. Constitutive G protein coupling profiles of understudied orphan GPCRs. *PLoS One* **2021**, *16*, No. e0247743.

(11) Uhlenbrock, K.; Gassenhuber, H.; Kostenis, E. Sphingosine 1-phosphate is a ligand of the human gpr3, gpr6 and gpr12 family of constitutively active G protein-coupled receptors. *Cellular signalling* **2002**, *14*, 941−953.

(12) Ballesteros, J. A.; Weinstein, H. (1995) Integrated methods for the construction of three-dimensional models and computational probing of structure-function relations in G protein-coupled receptors, In *Methods in neurosciences*, pp 366−428, Academic Press.

(13) Lin, X.; Li, M.; Wang, N.; Wu, Y.; Luo, Z.; Guo, S.; Han, G.-W.; Li, S.; Yue, Y.; Wei, X.; Xie, X.; Chen, Y.; Zhao, S.; Wu, J.; Lei, M.; Xu, F. Structural basis of ligand recognition and self-activation of orphan GPR52. *Nature* **2020**, *579*, 152−157.

(14) Xu, P.; Huang, S.; Guo, S.; Yun, Y.; Cheng, X.; He, X.; Cai, P.; Lan, Y.; Zhou, H.; Jiang, H.; Jiang, Y.; Xie, X.; Xu, H. E. Structural identification of lysophosphatidylcholines as activating ligands for orphan receptor GPR119. *Nature Structural & Molecular Biology* **2022**, *29*, 863−870.
(15) Yu, L.; He, L.; Gan, B.; Ti, R.; Xiao, Q.; Yang, X.; Hu, H.; Zhu, L.; Wang, S.; Ren, R. Structural insights into sphingosine-1-phosphate receptor activation. *Proc. Natl. Acad. Sci. U.S.A.* **2022**, *119*, No. e2117716119.
(16) Liang, J.; Inoue, A.; Ikuta, T.; Xia, R.; Wang, N.; Kawakami, K.; Xu, Z.; Qian, Y.; Zhu, X.; Zhang, A.; Guo, C.; Huang, Z.; He, Y. Structural basis of lysophosphatidylserine receptor GPR174 ligand recognition and activation. *Nat. Commun.* **2023**, *14*, 1012.
(17) Li, H.; Zhang, J.; Yu, Y.; Luo, F.; Wu, L.; Liu, J.; Chen, N.; Liu, Z.; Hua, T. Structural insight into the constitutive activity of human orphan receptor GPR12. *Sci. Bull.* **2022**, *68*, 05−104.
(18) Chen, G.; Staffen, N.; Wu, Z.; Xu, X.; Pan, J.; Inoue, A.; Shi, T.et al.Structural and functional characterization of the endogenous agonist for orphan receptor GPR3. *Cell Res.* **2024** DOI: 10.1038/s41422-023-00919-8.
(19) Xiong, Y.; Xu, Z.; Li, X.; Wang, Y.; Zhao, J.; Wang, N.; Duan, Y.et al.Identification of oleic acid as an endogenous ligand of GPR3. *Cell Res.* **2024**, DOI: 10.1038/s41422-024-00932-5.

https://doi.org/10.1021/acs.biochem.3c00647
Biochemistry 2024, 63, 625−631